Agricultural and Forest Meteorology 269–270 (2019) 157–168

Contents lists available at ScienceDirect

Agricultural and Forest Meteorology

journal homepage: www.elsevier.com/locate/agrformet

Terrestrial lidar scanning reveals fine-scale linkages between microstructure and photosynthetic functioning of small-stature spruce trees at the forest-tundra ecotone

Andrew J. Maguire[a,b,*], Jan U.H. Eitel[a,b], Lee A. Vierling[a,b], Daniel M. Johnson[c], Kevin L. Griffin[d,e], Natalie T. Boelman[d], Johanna E. Jensen[e], Heather E. Greaves[f], Arjan J.H. Meddens[a]

[a] Department of Natural Resources and Society, University of Idaho, Moscow, ID 83844-1139, USA
[b] McCall Outdoor Science School, University of Idaho, McCall, ID, 83638, USA
[c] Warnell School of Forestry and Natural Resources, University of Georgia, Athens, GA, USA
[d] Department of Earth and Environmental Sciences, Lamont-Doherty Earth Observatory, Columbia University, New York, NY, USA
[e] Department of Ecology, Evolution, and Environmental Biology, Columbia University, New York, NY, USA
[f] Institute of Arctic Biology, University of Alaska Fairbanks, Fairbanks, AK, USA

ARTICLE INFO

Keywords:
Microstructure
Microtopography
Forest-tundra ecotone
Northern treeline
Lidar
Chlorophyll fluorescence

ABSTRACT

The forest-tundra ecotone (FTE) is exhibiting myriad responses to rapid environmental change. Microstructural variability (at cm to m length scales) of vegetation canopies and geomorphic features may modulate the response of FTE vegetation to regional climate changes. Understanding the influence of microstructure on tree function at the FTE is particularly relevant during vulnerable early growth stages. During these stages, individual trees are tightly coupled to conditions of the surface boundary layer, which can be more conducive to growth than the conditions above the boundary layer. Until recently, however, it has been difficult to characterize microstructure in a replicable, transferable manner. This study builds upon substantial research on ecological responses of trees at the FTE to growth environment conditions by integrating high-resolution terrestrial lidar scanning (TLS) to characterize microstructure. Our main goal was to use TLS technology to understand the effects of microstructure on photosynthetic functioning (i.e., chlorophyll fluorescence) of small-stature white spruce (*Picea glauca* (Moench) Voss) trees at the FTE. Our specific objectives were to: 1) determine how much variance in photosynthetic functioning is explained by microstructure; 2) identify microstructural metrics that most strongly control variance in photosynthetic functioning; and 3) determine the scales at which microstructural metrics most strongly drive variance in photosynthetic functioning. Random Forest modeling demonstrated that 28% of variance in photosynthetic functioning can be explained through variation in fine-scale environmental conditions that are modulated by microstructure alone. Insolation and canopy roughness were the most important predictors of photosynthetic functioning, and the sensitivity of photosynthetic functioning to canopy roughness was scale-dependent. This suggests that microstructure affects spatial heterogeneity in the boundary layer that may influence carbon assimilation of small-stature spruce trees. This research emphasizes the importance of quantifying microstructure in study systems where fine-scale heterogeneity of the growth environment may modulate plant responses to regional climate change.

1. Introduction

The forest-tundra ecotone (FTE), the world's largest vegetation transition zone spanning 13,000 km across the northern hemisphere (Callaghan et al., 2002a), is inherently responsive to fine-scale changes in environmental conditions (Sveinbjörnsson et al., 2002). The FTE is defined by its transition from boreal forest to treeless arctic tundra (Payette et al., 2001). However, the distribution and biophysical structure of this transition are variable across scales (Callaghan et al., 2002a, 2002b; Payette et al., 2001). The Arctic-boreal zone is warming disproportionately faster than the global average (Kattsov et al., 2005; Post et al., 2009; Serreze et al., 2000) yet uncertainties persist regarding

* Corresponding author.
E-mail address: amaguire@uidaho.edu (A.J. Maguire).

https://doi.org/10.1016/j.agrformet.2019.02.019
Received 28 June 2018; Received in revised form 9 November 2018; Accepted 11 February 2019
Available online 15 February 2019

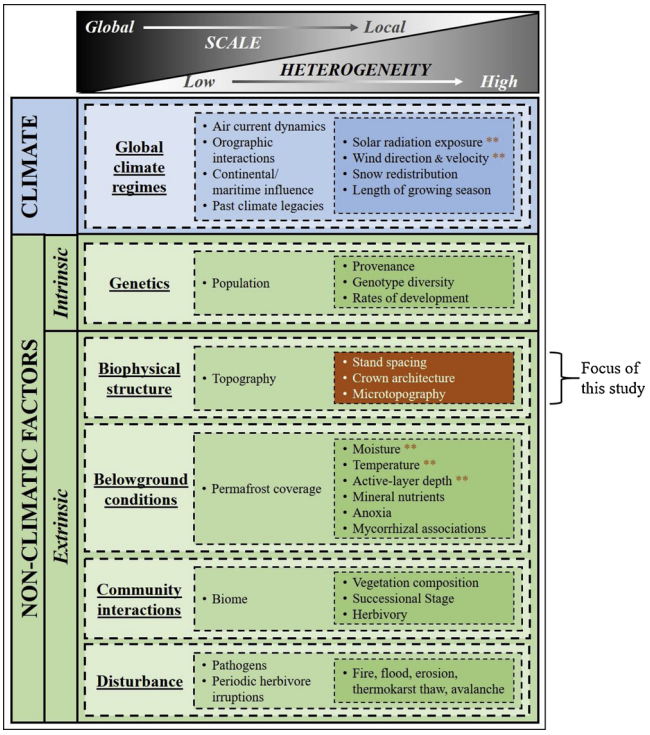

Fig. 1. A conceptual framework of the modulating effects fine-scale factors have on coarse-scale factors that drive photosynthetic functioning of small-stature trees at the FTE, adapted from Holtmeier and Broll (2017b). The focus of this study is biophysical structure at fine scales (orange box). Asterisks (**) indicate other elements that microstructure may indirectly affect.

how trees within the FTE may respond to environmental change (Holtmeier and Broll, 2007, 2005; Skre et al., 2002; Trant and Hermanutz, 2014; Woods, 2014). Contributing to this uncertainty are factors that might modulate impacts from climate change, such as biophysical structure of vegetation and terrain.

Along with climate variables, plant function at the FTE is responsive to a range of intrinsic conditions (e.g., genetics) and extrinsic conditions (e.g., biophysical structure, belowground conditions, community interactions, and disturbance) that hold influence from coarse to fine scales (Fig. 1). It is well-established that macrostructural features (i.e., vegetation canopy and topography at decameter to kilometer scales) drive environmental conditions and consequently exert controls on local vegetation distribution, structure, and function (Brown, 1994; Danby and Hik, 2007; Ropars et al., 2015; Ropars and Boudreau, 2012; Shaver et al., 1996; Zong et al., 2014). Mounting evidence suggests that microstructure (i.e., vegetation canopy and topography at cm to m scales) may be important for modulating environmental conditions to which plant processes are sensitive (e.g., temporal variance in intensity and duration of solar radiation, Pearcy, 1990; Smith et al., 1989; Smith and Berry, 2013; Way and Pearcy, 2012). For example, recent research on alpine snowbed plant communities demonstrates that local-scale heterogeneity in microstructure drives fine-scale variation in the growth environment, which in turn affects plant phenology (Domènech et al., 2016). Moreover, interactions between climate and local microstructure lead to steep gradients in plant function across fine spatial scales (Chaudhary et al., 2018; Holtmeier and Broll, 2017a; Yang et al., 2012). Indeed, Scherrer and Körner demonstrated that microtopography can facilitate thermal gradients at the surface mimicking those observed over broad elevational or latitudinal ranges (2010) and can drive alpine plant diversity (2011). Further, considerable research has described the influence of microtopography on soil dynamics (Born et al., 2015; Holtmeier and Broll, 1992) and wind dynamics (Greenwood et al., 2015, 2014; Holtmeier and Broll, 2010) that drive spatial patterns of tree establishment, growth, and survival.

Microstructure may be of particular importance to the function of small-stature trees due to its strong controls on fine-scale variations in the surface boundary layer and hydrology (Geiger et al., 2003; Germino et al., 2002; Germino and Smith, 1999; Johnson et al., 2011; Kambo and Danby, 2018; Sullivan and Sveinbjörnsson, 2010). During early growth stages, trees often rely on boundary layer conditions conducive to growth (Körner, 2012, 1998) that decouple them from harsher, more variable atmospheric climate conditions. The importance of a protective boundary layer during the growing season may be especially relevant in the context of immature tree development within the FTE, the ecological threshold of tree establishment (Holtmeier and Broll, 2007; Resler et al., 2005; Resler, 2006). Research on latitudinal and alpine treelines suggests that microstructure regulates the mechanical influence of wind on tree physiognomy and the physiological influence of wind on transpiration along with the indirect effects from snow accumulation (Anschlag et al., 2008; Baig and Tranquillini, 1980; Holtmeier and Broll, 2010, 2017a; Tranquillini, 1979). Moreover, sheltering from wind by neighboring vegetation canopies has been highlighted as being particularly important for the facilitation of immature tree establishment and survival (Holtmeier, 2009; Holtmeier et al., 2003; Holtmeier and Broll, 2010, 2007; Resler et al., 2005). Exposure to solar radiation, governed by microtopography and proximity to vegetation canopies, can drive spatial heterogeneity in photoinhibition of immature trees (Germino et al., 2002; Germino and Smith, 1999; Smith et al., 2003). Furthermore, Sullivan and Sveinbjörnsson (2010) demonstrated that microstructure (e.g., tussocks and frost boils) affected fine-scale variation in soil temperature and volumetric soil water content, consequently regulating seedling establishment and growth at the northern edge of the FTE.

The above studies demonstrate a clear effect of microstructure on the function of immature trees, though many rely on simple manual measurement approaches that may not fully capture the complexities of microstructure. Hence, prior research may overlook linkages important for understanding how microstructure may modulate climate change effects on the FTE. To further disentangle the complex relationships between microstructure, growth environment, and plant function, replicable and transferable approaches for quantifying heterogeneity in microstructure are required (Yang et al., 2012). One technology that could fill this void is terrestrial lidar (light detection and ranging) scanning (TLS). This laser-based technology enables resolution of 3-dimensional (i.e., x, y, z) structure at cm-level detail and has facilitated novel insights into ecological processes controlled by microstructure, including canopy light environment and radiative transfer modeling (Bittner et al., 2012; Magney et al., 2016, 2014; Rosskopf et al., 2017; Widlowski et al., 2014), geomorphic processes (Eitel et al., 2011; Sankey et al., 2011), spatial patterns of aboveground biomass (Clawges et al., 2007; Greaves et al., 2017, 2015), and myriad other applications (reviewed in Eitel et al., 2016). Based on the 3-dimensional structural information provided by TLS, a range of ecologically important structural metrics can be derived that have been demonstrated as ecologically important such as ground surface or vegetation canopy roughness, solar radiation, and wind shelter (Holtmeier and Broll, 2007, 2005; Sullivan and Sveinbjörnsson, 2010). In addition, since structure-to-function relationships are inherently scale-dependent (Haubrock et al., 2009; Huang and Bradford, 1990; Phillips, 1995; Shepard et al., 2001), the highly resolved structural information from TLS may allow researchers to determine the most important scales at which microstructural metrics drive variance in plant function.

The overarching goal of this study was to use TLS technology to explore relationships between microstructure and photosynthetic functioning of small-stature spruce trees growing at the FTE. Photosynthetic functioning, which encompasses the capacity of foliar photosystems to support CO_2 assimilation, can be estimated using chlorophyll *a* fluorescence (ChlF), an optically sensed signal of photosynthetic electron transport that is sensitive to both light use efficiency

and absorbed photosynthetically active radiation (APAR) (Porcar-Castell et al., 2014). ChlF provides information about processes such as photochemistry, metabolism, and heat dissipation (Ball et al., 1995; Maxwell and Johnson, 2000), but also may be indicative of plant stress levels (Krause and Weis, 1991; Maxwell and Johnson, 2000). ChlF is a well-established proxy for plant function (Krause and Weis, 1991; Maxwell and Johnson, 2000) with the potential to link remotely sensed information to ecophysiological processes (Porcar-Castell et al., 2014), making it the ideal tool for this study.

Our specific objectives were to: 1) determine how much variance in photosynthetic functioning is explained by microstructure; 2) identify microstructural metrics that most strongly control variance in photosynthetic functioning and 3) determine the scales at which microstructural metrics most strongly drive variance in photosynthetic functioning. This study builds upon substantial research on physiological responses of trees at the FTE to growth environment conditions (Holtmeier and Broll, 2010; Nicklen et al., 2016; Sullivan and Sveinbjörnsson, 2010) by integrating very high-resolution remote sensing tools. Outcomes of this study will provide insight on how remotely sensed fine-scale structural information can improve the interpretation of ecological signals at the FTE.

2. Materials and methods

2.1. Study site

Field data were collected at four plots along an approximately 3 km north-south transect within the forest-tundra ecotone (FTE) near the Dalton Highway (68° 0′ N, 149° 45′ W, 730 m elevation), Alaska, USA on the southern side of the Brooks Range, 100 miles north of the Arctic Circle (Fig. 2a-b). Traveling north along this transect, trees become increasingly sparse and the landscape eventually transitions into treeless tundra. Mean annual precipitation and air temperature for the study area averaged from two nearby SnowTelemetry (SNOTEL) sites at Atigun Pass (68° 08′ N, 149° 29′ W, 1463 m elevation) and Coldfoot (67° 15′ N, 150° 11′ W, 317 m elevation) from 2009 through 2017 are 521.5 mm and -5.9 °C, respectively. The brief growing season is approximately 12 weeks (McNab, 1996). Here, the FTE is underlain by continuous permafrost and consists of both black spruce (*Picea mariana* (Mill.) BSP) and white spruce (*P. glauca* (Moench) Voss) along with arborescent willows (*Salix* spp.) growing in the wettest areas. Low-stature deciduous shrubs (e.g., *Betula nana* L., *Alnus* sp., *Salix* spp.), sedges (e.g., *Eriophorum* spp.), and mosses dominate the understory. Topography is variable across multiple spatial scales: situated in a valley along the Dietrich River, trees grow in a band along the floodplain and gently sloping lower elevations before tundra vegetation dominates at only mildly higher elevations (Fig. 2c). Trees cease to occur on the south side of the of the Brooks Range divide.

2.2. Field data collection

Four study plots, each approximately 1600 m^2 in area, were established in mid-June 2016. Plot locations were selected adjacent to stands of mature spruce trees, at the tree-limit (*sensu* Holtmeier and Broll, 2005). Plots were spread along a north-south transect to sample the variance in photosynthetic functioning and microstructure of the FTE in this study site. Approximately 20 small-stature (i.e., < 2 m height) white spruce (*P. glauca*) trees were selected within each plot for a total of 82 trees across all study plots. To assess photosynthetic functioning of spruce trees, three bundles of needles in the upper-part of each tree crown were dark-adapted in situ using aluminum foil over leaf clips for 25 min prior to ChlF measurement. Dark-adapted ChlF measurements were collected at around solar noon using an Optisci OS30p+, a pulse modulated fluorometer employing a red actinic light (Opti-Sciences, Inc. Hudson, New Hampshire, USA) at a saturating light intensity of 3500 μmol m^{-2} s^{-1}. We selected a widely used parameter of ChlF, F_v/F_m (i.e., the ratio of variable fluorescence to maximum fluorescence, measuring the potential quantum efficiency of photosystem II), as an indicator of photosynthetic performance (Baker, 2008; Maxwell and Johnson, 2000). A minimum threshold of F_v/F_m for non-stressed leaves has been consistently reported as 0.83, which we used as a standard for inference (Björkman and Demmig, 1987 in Baker, 2008). The average F_v/F_m value for the three needle bundles was used as the response value for each tree.

2.3. Terrestrial lidar scanning and preprocessing

Terrestrial lidar scanning (TLS) data were acquired with a Leica ScanStation C10 (Leica Geosystems Inc., Heerbrugg, Switzerland). This time-of-flight 532 nm (green wavelength) laser instrument has a scan rate of up to 50,000 returns s^{-1}, a maximum sample density exceeding 1 mm^{-1}, and a maximum range of 134 m at 18% albedo. The nominal distance accuracy is 4 mm and nominal position accuracy is 6 mm. The low beam divergence (0.14 mrad) of the green scanning TLS instrument ensures that the laser frequently penetrates the canopy to measure the ground surface, which is important for characterizing microtopography. In mid-June 2016, concurrent with ChlF sampling, study plots were scanned from three to five different positions to minimize occlusion by vegetation canopies and maximize the spatial extent of point clouds. Using common locations from reflectance targets, the point clouds from different scan positions were registered into a single point cloud using Cyclone 9.1 (Leica Geosystems Inc., Heerbrugg, Switzerland). The point cloud was then georegistered using GPS data collected from a Trimble R7 and an external Zephyr geodetic antenna with nominal vertical and horizontal accuracy of 5 mm (Trimble Inc., Dayton, OH, USA). Tree locations were marked in the field using cardboard signs for identification in scan images and to link with respective ChlF measurements. UTM coordinates for each of the 85 trees were manually extracted from the georegistered TLS point cloud by identifying the coordinates of the laser return associated with the top of each tree crown. Point clouds were manually edited to remove spurious returns from incidental airborne particles and flying insects and were cropped to approximately 40 m x 40 m (Fig. 3).

Using the point cloud from each sample plot, 'ground' (lowest) and 'top-of-canopy' (highest) returns were extracted using a classification algorithm in R (R Core Team, 2017) developed for similar vegetation-related applications of lidar (Greaves et al., 2016, 2015). Because resolving a 'bare earth' surface in arctic ecosystems is complicated by the near-continuous moss layer and arctic soil matrix properties (e.g., slowly decomposing foliage and root biomass), this approach was used to characterize the surface underlying erect vegetation. As part of this algorithm, several parameters (ground return filter grid resolution, ground return neighborhood size, and canopy return filter grid resolution) must be optimized for given site conditions to obtain reliable classification results. For the optimization, 20 manually classified ground returns were identified in one plot by examining the TLS point cloud in conjunction with the images captured by the TLS instrument to identify locations of ground surface. These manually classified returns were compared against automatically classified ground returns across varying parameter values. Optimized 'ground' return algorithm parameter values had a coefficient of determination (r^2) of 0.973 for predicting ground height against manually classified ground returns. 'Ground' returns were identified by a double-pass algorithm, initially by applying a 0.1 m resolution grid to the point cloud and retaining only the lowest (z-coordinate) return within each grid cell. The second pass of the point cloud further refined the set of laser returns by selecting the return with the lowest z-coordinate of all nearest neighbors (neighborhood size of 9). 'Top-of-canopy' (z-coordinate) returns were identified by a single-pass algorithm by applying a 0.005 m resolution grid to the point cloud and retaining only the highest return within each grid cell. Based on our interest in characterizing the structural complexity of vegetation canopies within cm to m length scales, we selected a filter

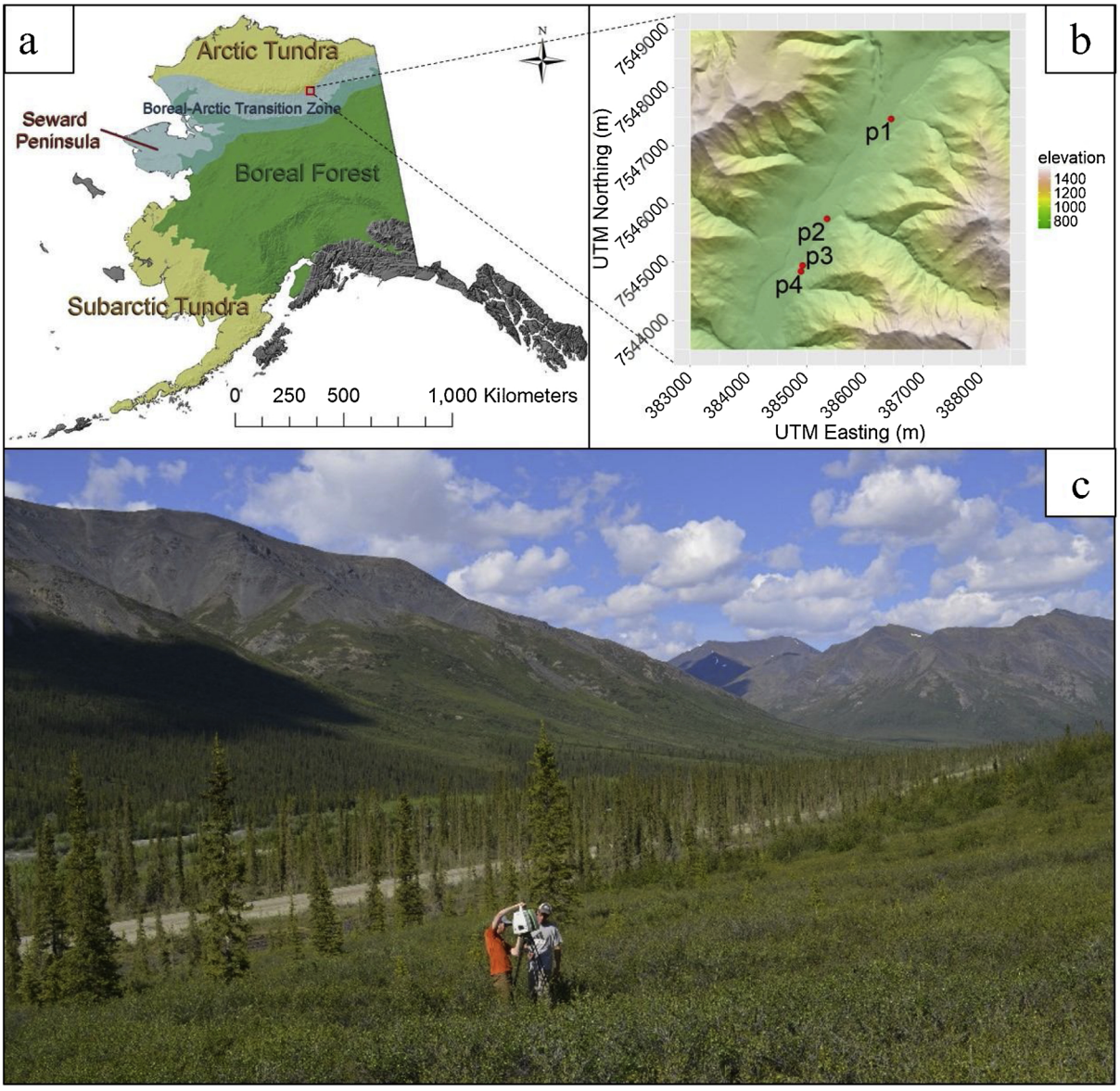

Fig. 2. A map of Alaska shows the boreal forest and tundra regions across the state (2a; credit: Alaska Science Center, USGS). The coarse-scale topographic positions of plots 1–4 are shown within the study region in the Brooks Range (2b). A perspective of one study plot at the forest-tundra ecotone with mature spruce trees transitioning into short-stature trees and low-stature deciduous shrubs (2c; photo credit: Kevin Krajick/ Lamont-Doherty Earth Observatory).

size that would detect fine-scale changes in canopy height typical of FTE vegetation. The remaining sets of 'ground' and 'top-of-canopy' laser returns were used to interpolate, respectively, bivariate digital terrain models (DTMs) and digital surface models (DSMs), which were rasterized at 0.10 m resolution using the 'raster' package (Hijmans, 2016) in R.

2.4. Derivation of microstructural metrics

All microstructural metrics were derived from georegistered TLS point clouds (Fig. 4). Ground roughness (m) and canopy roughness (m) were calculated as the standard deviation of the z-coordinates of laser returns classified as 'ground' or 'top-of-canopy', respectively. Slope (radians), aspect (radians from north), and curvature (m^{-1}) layers were created based on the average respective topographic values extracted from DTM pixels using the 'RSAGA' package (Brenning and Bangs, 2016) in R (R Core Team, 2017). Aspect values were cosine-transformed from radians to a continuous variable representing northeast – southwest facing aspects between 0–1 (Roberts and Cooper, 1989).

To characterize the wind environment at each tree location, a topographic wind shelter index (0–1) was calculated based on both the DTMs and DSMs using the 'RSAGA' package in R. The wind shelter index was calculated using a moving window that identified the highest elevation pixel as a sheltering feature from a horizontal wind direction, searching out along either the DSM or DTM for a prescribed length of pixels within a sector for elevational differences relative to the pixel of interest (i.e., tree location) (Plattner et al., 2006; Winstral et al., 2002). For the purpose of evaluating very fine-scale processes, we used a wind radius (search length) of one pixel (0.10 m). Based on data collected by 10 nearby (20–500 m) anemometers (METER Group, Inc., Pullman, WA, USA) from June to September 2016 the mean wind direction (149° from North) and directional tolerance (60°) were used as parameters for the wind shelter calculations. Wind data were not available outside of the growing season (September – April) at this site, but these data should be considered representative of the wind environment during ChlF sampling.

Insolation was modeled using the 'insol' package (Corripio, 2015) in R. This function considers geographic position, solar geometry during

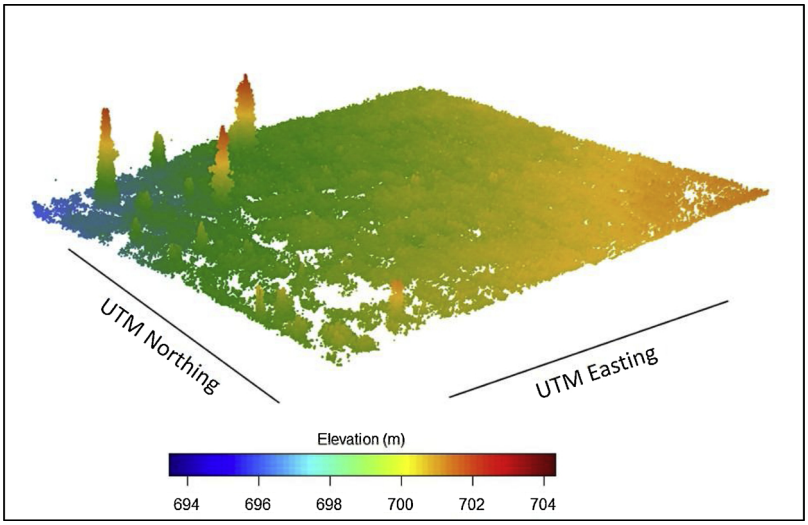

Fig. 3. A visualization of one georegistered point cloud (Plot 3) illustrating the high-resolution biophysical structural information from terrestrial lidar scanning data acquisition.

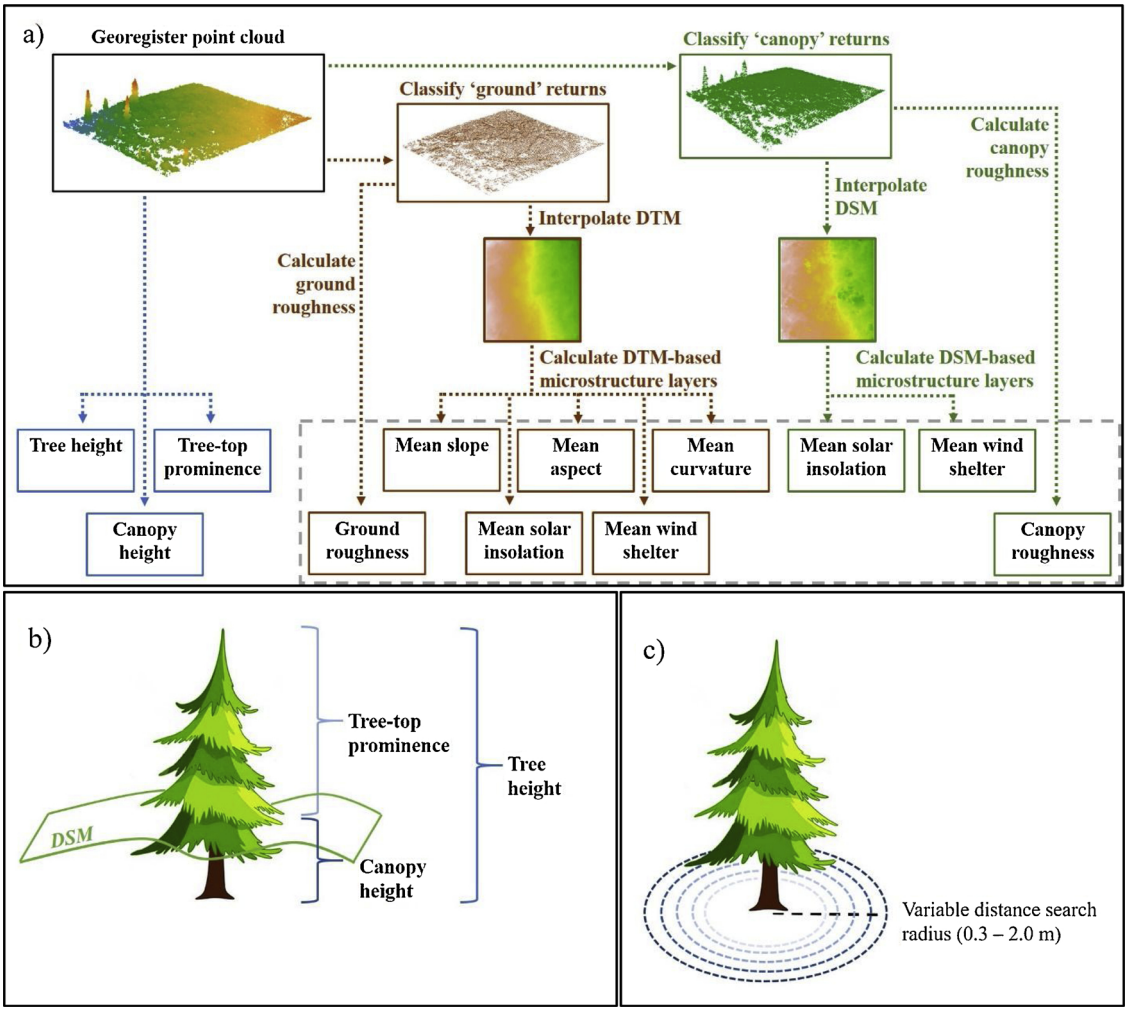

Fig. 4. Conceptual model of the derivation of terrestrial lidar scanning-derived metrics used to characterize the microstructure around small-stature white spruce trees at the forest-tundra ecotone (4a); extraction of three vegetation-structure metrics (4b); and the extraction of nine microstructural metrics (indicated by gray dashed box in 4a) at search radii 0.3–2.0 m around small-stature spruce trees (4c).

the period of interest, and atmospheric conditions to calculate direct and diffuse solar radiation across a rasterized surface. Values for atmospheric parameters (e.g., visibility, ozone thickness, albedo, relative humidity, and air temperature) for insolation modeling were retrieved from NOAA North American Regional Reanalysis (NARR) data (Mesinger et al., 2006). Insolation was calculated at five minute timesteps for 10 days prior to the final sampling date (15–24 June 2016), to assess dynamics in insolation over a period relevant to observed ChlF measurements. Three separate layers were calculated to account for the effects of landscape topography on local light environment (e.g., occluding or amplifying effects of hillslopes). A "local insolation" layer was derived by inputting the 0.10 m resolution DTMs and DSMs for each approximately 1600 m^2 TLS plot. Next a "landscape insolation" layer was derived using the Arctic DEM 5 m resolution product (Polar Geospatial Center, 2017), cropped to a 30 by 40 km extent, to account for the influence of broad scale topography of the mountainous terrain of the Brooks Range. A "flat insolation" layer was derived at the same resolution (5 m) as the "landscape insolation" layer, with all topography removed using the 'raster' package in R. This allowed for the calculation of default insolation based solely on geographic position, solar geometry, and atmospheric conditions, without the influence of topography. A landscape-correction factor ranging in value from 0.21 to 5.97 was calculated by dividing the "landscape insolation" layer by the "flat insolation" layer (per five-minute time step, per 5 m grid cell). This matrix of landscape correction factors was applied to the associated 0.10 m grid cells of both the DTM- and DSM-based "local insolation" layers to derive a final corrected local insolation layer (J m^{-2}). This approach allowed for the focus of this insolation layer to remain in the context of microstructure without ignoring the effect of landscape-scale topography on insolation.

Given our focus on the effects of microstructure on plant function, the aforementioned microstructural metrics were extracted within a variable 0.3–2.0 m search radius (0.1 m increment) from each tree location. The minimum search radius at which all microstructural metrics could be derived for each tree was 0.3 m. Mean values of the pixels within a given search radius were recorded from each respective microstructural metric layer.

In addition, we derived three vegetation-structure metrics: tree height (i.e., vertical difference between z-coordinate values of the manually classified 'top-of-canopy' laser return of tree crown and the 'ground' laser return of tree stem), tree-top prominence (i.e., vertical difference between the z-coordinate value of 'top-of-canopy' return of tree crown and the value of the collocated DSM pixel), and canopy height (i.e., difference between respective DSM and DTM pixel collocated with each tree).

2.5. Data analysis

We used Random Forest (RF) to model photosynthetic functioning (i.e., F_v/F_m) using the microstructural metrics (nine metrics measured at 18 scales along with tree height, tree-top prominence, canopy height, and UTM Easting and Northing for a total of 167 covariates). RF is a non-parametric machine learning approach that allows for efficient handling of data with many predictors relative to the number of observations, with each individual predictor providing limited information (Breiman, 2001). The RF approach combines many regression trees, each grown using a random subset of predictors and observations. RF is robust to overfitting and to multicollinearity because it uses a subset of predictors for each regression tree, hence retaining the ability to quantify importance of multiple highly collinear predictors by distributing variable importance across all correlated predictors (Belgiu and Drăgu, 2016; Cutler et al., 2007; Dormann et al., 2013). Because RF is non-parametric, the modeling framework makes no assumptions of the distribution or independence of predictor and response variables (Cutler et al., 2007). As our goals were: 1) to determine how much total variance in F_v/F_m can be explained by microstructural metrics and 2) to quantify the importance of each predictor variable across scales, we did not reduce our model to include only predictor variables that are below a certain correlation threshold (e.g., $r^2 = 0.9$ in Genuer et al., 2010). The RF model provides an estimation of variance explained by the input predictors, which addresses our first objective, and RF provides estimates of variable importance, based on increase in mean squared error of each regression tree when a given variable is permuted while all others remain unchanged (Genuer et al., 2010; Liaw and Wiener, 2002), which addresses our second and third study objectives.

To run RF models, we used the package 'randomForest' (Liaw and Wiener, 2015) in R, with the default settings for both *mtry* (i.e., the number of predictors sampled at each node: 1/3 of total predictors) and *ntree* (i.e., the number of regression trees grown for each run of RF: 500). Because this package outputs average variable importance estimates for each forest rather than the distribution across regression trees within a forest, the RF algorithm was executed 100 times to account for the inherent stochasticity of variable importance scores (Liaw and Wiener, 2002; Millard and Richardson, 2015) and to provide a range of variable importance for interpretation. This approach is equivalent executing RF to grow 50,000 regression trees. Variable importance estimates were subsequently converted to a ranking following each execution of the RF algorithm ($n = 100$), due to the relative stability of rankings over raw importance estimates across executions of RF (Liaw and Wiener, 2002). We report the distribution of the different ranks for each variable to present a final distribution of importance of each microstructural metric.

3. Results

Field sampling indicated that all 82 white spruce trees were below the minimum threshold for unstressed foliage (i.e., mean F_v/F_m values < 0.83; Fig. 5). A Kruskal-Wallis one-way analysis of variance indicated that photosynthetic functioning of spruce trees, measured by

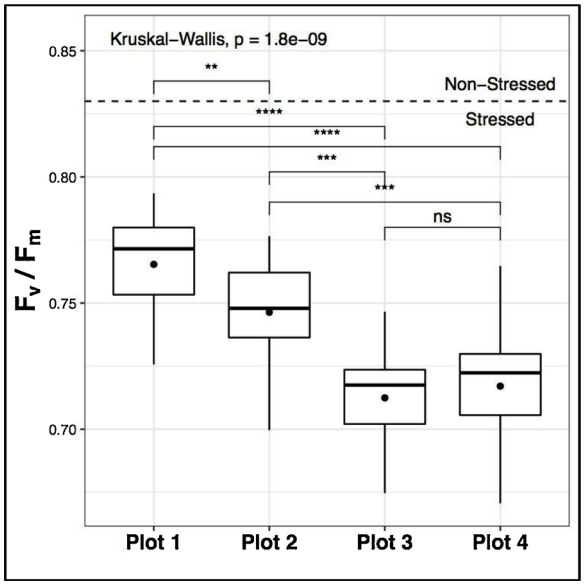

Fig. 5. Distribution of mean F_v/F_m values from three needle bundles each for 82 small-stature white spruce trees across four sample plots ($n_1 = 22$, $n_2 = 18$, $n_3 = 18$, $n_4 = 24$) at the forest-tundra ecotone. Boxes display the first quartile, median, and third quartile, whiskers display the range of each sample plot, and dots indicate the mean value of each sample plot. Kruskal-Wallis was used to test for significant difference in F_v/F_m values across all plots ($p = 1.8 * 10^{-9}$) and between plots (pairwise comparisons indicated with the symbols: ns: $p > 0.05$; ** $p < 0.01$; *** $p < 0.001$; **** $p < 0.0001$;). The threshold of $F_v/F_m = 0.83$ was used to assess whether foliage was considered stressed ($F_v/F_m < 0.83$) or non-stressed ($F_v/F_m > 0.83$) (Björkman and Demmig, 1987 in Baker, 2008).

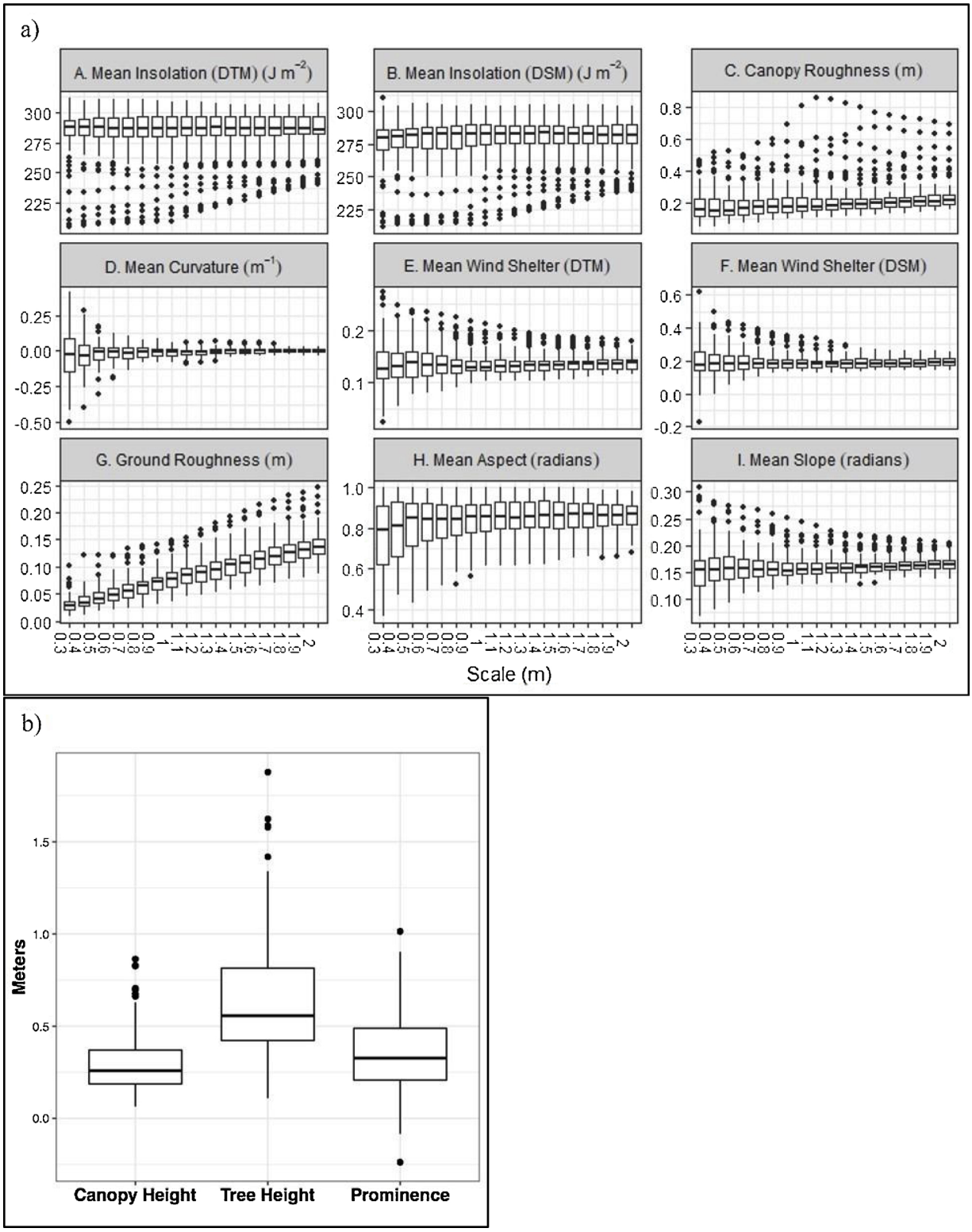

Fig. 6. Distribution of observed values of scale-dependent microstructural metrics (6a) and scale-independent vegetation-structure metrics (6b) derived from terrestrial lidar scanning. Note: wind shelter is a dimensionless index.

F_v/F_m, varied significantly ($\alpha = 0.05$) across all plots along the north-south transect, as well as between each pairwise comparison of plots except Plots 3 and 4. Interestingly, trees growing at the most northern location, Plot 1, were the least stressed, with mean $F_v/F_m = 0.77$ ($n_1 = 22$), followed by Plot 2 with mean $F_v/F_m = 0.75$ ($n_2 = 18$). Located at approximately the same latitude along the north-south transect, Plots 3 and 4 were the most stressed with mean $F_v/F_m = 0.71$ ($n_3 = 18$) and $F_v/F_m = 0.72$ ($n_4 = 24$), respectively.

Distributions of scale-dependent microstructural metric values derived from TLS point clouds and subsequently interpolated DTMs and DSMs are shown in Fig. 6a. Observed values of mean insolation (DTM- and DSM-based), mean curvature, mean wind shelter (DTM- and DSM-based), mean aspect, and mean slope were increasingly homogeneous at broader search radii. Mean canopy roughness and mean ground

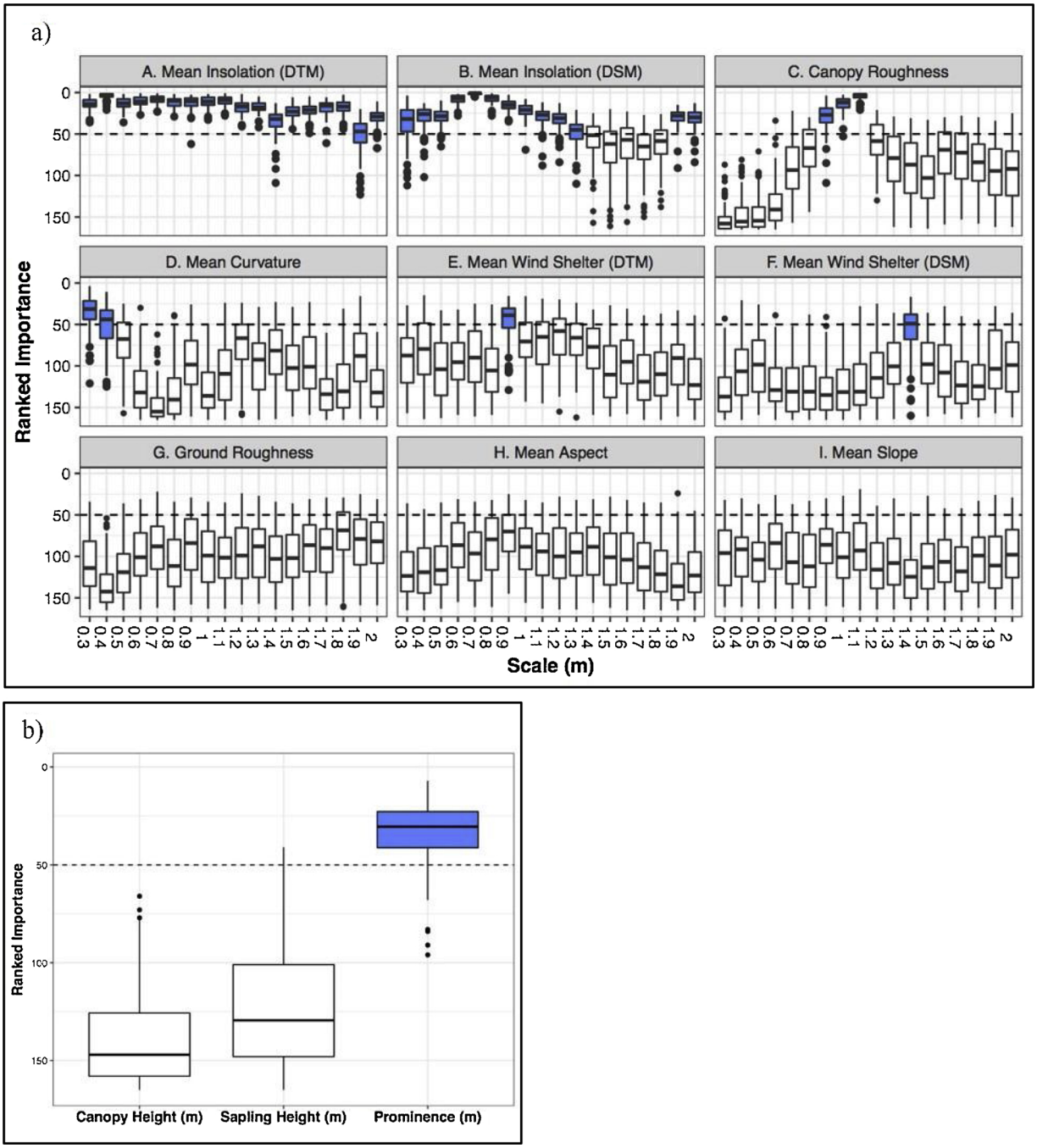

Fig. 7. Distribution of ranked importance values of scale-dependent microstructural metrics (7a) and scale-independent vegetation-structure metrics (7b) for explaining variance in photosynthetic functioning (i.e., F_v/F_m) of small-stature white spruce trees at the forest-tundra ecotone from 100 executions of the Random Forest (RF) algorithm run with 165 microstructural metrics (i.e., excluding UTM Easting and Northing). Ranked importance value of 1 indicates the upper limit (i.e., most important microstructural metric) possible for the RF algorithm. The most important microstructural metrics (i.e., median ranked importance value > 50) are displayed in blue. (For interpretation of the references to colour in this figure legend, the reader is referred to the web version of this article).

roughness increased in value and were increasingly heterogeneous in distribution at broader search radii. Tree height values ranged from 0.11 – 1.88 m. Tree-top prominence values showed that six of 82 trees were entirely below the surface of the canopy layer (i.e., negative values; Fig. 6b).

Using RF, microstructural metrics alone (i.e., excluding UTM Easting and Northing) explained a mean of 28% (SD = 1%) of the variance in F_v/F_m across 100 executions of the algorithm. When we included UTM Easting and Northing to account for the spatial distribution of sites along with microstructural metrics, this suite of variables explained a mean of 42% (SD = 1%) of the variance in F_v/F_m across 100 executions of the algorithm. The distribution of ranked importance of microstructural metrics by RF (excluding UTM Easting and Northing; Fig. 7) demonstrates that insolation at both the ground surface (i.e., DTM) and the canopy surface (i.e., DSM) along with canopy roughness were the most important microstructural attributes for explaining variance in F_v/F_m of small-stature white spruce trees. Results from the RF modeling also indicated that the importance of microstructural metrics in explaining variance in F_v/F_m are scale-dependent, though the degree to which they are scale-dependent differed among microstructural metrics. Insolation at the ground surface and the canopy surface were ranked as highly important (i.e., mean rank of

importance < 50) at nearly all scales. Interestingly, canopy roughness was only ranked as highly important at a narrow range of scales (0.9–1.1 m), whereas it was ranked in the lower range of importance (i.e., mean rank of importance > 50, or the top 36 predictor variables) at finer scales (0.3 – 0.6 m), suggesting that the sensitivity of F_v/F_m to canopy roughness is scale-dependent. Slope ranked in the lower range of importance across all scales, displaying minimal scale-dependence.

4. Discussion

4.1. The role of microstructure in modulating photosynthetic functioning

Photosynthetic functioning is affected by myriad factors beyond climate, such as genetics, biophysical structure, belowground conditions, community interactions, and disturbance (Fig. 1). Notable among these factors, research has demonstrated that biophysical structure at the micro-scale (cm to m length) is important in modulating coarse-scale climate conditions at vegetation transition zones to which plant function is responsive (Chaudhary et al., 2018; Holtmeier and Broll, 2017a; Yang et al., 2012). Hence it is consistent with these studies that we demonstrated that microstructural metrics alone explained 28% of the variance in F_v/F_m of small-stature white spruce trees at the forest-tundra ecotone (FTE). The observed 14% increase in variance explained by including UTM Easting and Northing as predictors in the RF algorithm suggests that plot-level effects are clearly important to photosynthetic functioning of the study trees. Such plot-level effects may include attributes of the local growth environment not captured by TLS-derived microstructure. In particular, provenance (i.e., acclimation of plants to the local conditions specific to their seed source) may be a possible driver of tree photosynthetic functioning. Prior research on plasticity in growth and leaf morphology of plants across elevational gradients has demonstrated the importance of provenance (Vitasse et al., 2014), suggesting provenance may be a driver of physiological variation along the latitudinal gradient observed in the present study. Although it seems plausible that the degree to which microstructure is important in modulating photosynthetic functioning of small-stature spruce trees varies across the FTE gradient, forming inferences on that dynamic for trees occurring outside the ecotone exceeds the scope of this study. The three most important microstructural attributes, canopy roughness and insolation at both the ground and canopy surfaces, could be interpreted as representing heterogeneity in both thermal and illumination properties of the growth environment. Empirical research has demonstrated that microstructure drives spatial heterogeneity in thermal microclimates (Scherrer et al., 2011; Scherrer and Körner, 2011, 2010). Our research complements this finding by demonstrating that photosynthetic functioning is sensitive to microstructure, particularly in the context of fine-scale spatial heterogeneity of solar radiation. Because of the unique light environment of the Arctic summer (continuous daylight throughout the growing season, solar azimuth angles at or approaching 360°, and high solar zenith angles), photosynthetic functioning has a nonlinear response to changes in solar radiation (Fernández-Marín et al., 2018; Gross, 1982). Moreover, because these trees do not experience dark periods during the growing season, it is likely that heterogeneity in biophysical structure provides diurnally recurring periods of reduced direct insolation that may be physiologically important to photosynthetic functioning (Pearcy, 1990; Smith et al., 2003, 1989; Smith and Berry, 2013; Way and Pearcy, 2012). Empirically based insights into a similar vegetation system, low stature deciduous shrubs in the Arctic, has illuminated the importance of the unique light environment of this region for driving within-crown partitioning in photosynthetic functioning (Magney et al., 2016). The sensitivity of photosynthetic functioning at the FTE to fine-scale spatial variation in insolation suggests that this metric may characterize both gradients of light exposure and thermal microclimates. The characterization of thermal microclimates may be further refined by integrating canopy roughness, which may modulate energy partitioning to a degree that facilitates or inhibits photosynthetic functioning. If canopy roughness is positively correlated to canopy density or aggregate surface area of foliage, and hence capacity for increased evapotranspiration, increased canopy roughness may bias the flux of energy toward latent over sensible pathways (Gersony et al., 2016; Stoner and Miller, 1975). Consequently, this may propel divergence in the roles played by physiological processes (e.g., water transport) that mechanistically underlie photosynthetic functioning. The evidence we present here on the sensitivity of small-stature spruce trees at the FTE to microstructure corroborates the well-established importance of boundary layer effects on small-stature plants (Howe et al., 2003; Johnson et al., 2011) as critical drivers of photosynthetic functioning. Under the potentially stressful conditions and abbreviated growing season of the FTE, small-stature trees are influenced by boundary layer dynamics, as they are more coupled to these adjacent growth environments than are large-stature trees. Tree-top prominence, the most important of the three vegetation-structure characteristics included in the RF analysis, may relate to the degree to which the tree crowns were decoupled from the boundary layer, as upper crown foliage is likely to interact with the free atmosphere. The importance of canopy roughness suggests that fine-scale canopy heterogeneity at the FTE may be important for facilitating turbulence of the atmosphere, thus disrupting the uniformity of the thermal profile of the sub-canopy boundary layer (Geiger et al., 2003; Johnson et al., 2011; Lambers et al., 2008), and increasing the importance of convection in driving overall energy partitioning. Surprisingly, given the abundance of wind-related research at ecotones, we did not observe that wind shelter was important in driving photosynthetic functioning of small-stature trees. This may indicate that the wind shelter index used here, originally designed to model snow redistribution across broad spatial scales (Plattner et al., 2006; Winstral et al., 2002), cannot sufficiently represent the comprehensive wind environment or its fine-scale interaction with microstructure at the level of interest for this study. Alternatively, our observation that a coarse-scale wind shelter index was of limited importance to photosynthetic function may indicate that this attribute is less important than fine-scale heterogeneity in boundary layer air flow, which we did not directly model.

It is worth noting that several of the microstructural metrics may provide useful, albeit indirect, inference for subsurface properties undoubtedly important in governing photosynthetic functioning at the FTE. Microstructure influences spring snowmelt dynamics, which in turn regulates soil temperature and moisture (Scherrer and Körner, 2011, 2010). Disagreements persist over the role of soil conditions in tree distribution and physiological condition at latitudinal treeline environments (Du, 2016; McNown and Sullivan, 2013; Sullivan, 2016; Sullivan et al., 2015); however, recent research suggests that soil temperature is a primary driver of fall photosynthetic phenology in this same study region (Eitel et al., 2019), which indicates that modulation of climate change-induced warming of soil temperature by microstructure may have substantial consequences on phenological changes to the FTE.

4.2. Further considerations

Our selected response variable, F_v/F_m, while ubiquitous in many studies on plant physiology, does have limitations for inferring photosynthetic functioning (Maxwell and Johnson, 2000). This ChlF variable is temporally constrained, hence it cannot be interpreted as an integrated response to all-season conditions. Rather, this response must be interpreted in the context of summer growth environment. This hampers our ability to infer the role of microstructure in mediating winter conditions, including snow depth and persistence, active layer depth and thaw timing, and the abrasive and damaging effects of low temperatures and wind on foliar biogeochemical properties covarying with photosynthesis. Photoinhibition, which likely occurs in all seasons (except during the continuous darkness of the Arctic winter) at the FTE

(Danby and Hik, 2007; Slot et al., 2005), may have lasting impacts that cannot be revealed with the selected response variable, but may enact irreversible damage (Germino and Smith, 1999). It is unclear from the present study how small-stature trees growing at the FTE may interact with microstructure to mediate photoinhibition. In addition, despite our lack of direct measurements of belowground conditions (e.g., soil nutrients or mycorrhizae), we expect soil moisture and soil temperature to covary with microstructural metrics (Scherrer and Körner, 2011, 2010), and it is likely that each of these belowground covariates affects photosynthetic functioning (Fig. 1; Germino et al., 2006). Research has suggested that interactions between shrub cover and topography influence immature tree establishment and growth (Kambo and Danby, 2018) as well as physiological condition at treeline ecotones (Germino and Smith, 1999; Maher et al., 2005); however, our study did not comprehensively quantify shrub structure (i.e., beyond the elements of shrub cover characterized by canopy roughness and canopy height) to provide evidence of associations between shrubs and photosynthetic functioning of immature trees at the FTE. Whereas the primary goal of modeling insolation was to understand the interaction of microstructure and solar geometry, with reduced emphasis on atmospheric parameters of this model (i.e., visibility, ozone thickness, relative humidity, and air temperature), it is worth noting that fine-scale spatiotemporal variance in surface parameters (e.g., albedo) within our study plots was not captured by the NARR data used in the model. Finally, our use of RF for assessing the role of microstructure in driving photosynthetic functioning presents issue for interpreting ecological relationships. Because RF does not reveal specific statistical relationships, we could not quantify the direction or magnitude of observed associations between microstructural attributes and photosynthetic functioning.

4.3. Recommendations for further research

The findings of this study present a compelling case for the importance of microstructure to the photosynthetic functioning of small-stature trees growing at the FTE. However, further investigation is warranted to address the limitations of this study and to discern a more comprehensive understanding of the nuanced relationships discussed herein. First, we suggest that integrating thermal imagery, near-surface anemometers, soil temperature and moisture sensors, and air temperature sensors with the highly resolved structural information available from terrestrial laser scanning, would allow for characterization of microclimatic heterogeneity near the ground (i.e., boundary layer conditions) in relation to microstructural metrics. Next, because the response variable we selected (i.e., F_v/F_m) was interpreted as a proxy of photosynthetic functioning, we recommend assessing the relationship between ChlF parameters (namely F_v/F_m) and carbon assimilation (e.g., via foliar gas exchange) to better characterize photosynthetic functioning of trees growing at these sites. Moreover, we also suggest that measurements of non-photochemical quenching (i.e., the efficiency by which ChlF yield is reduced through heat dissipation) and photochemical quenching (i.e., the efficiency by which ChlF yield is reduced through photosynthesis) would provide an opportunity to mechanistically understand the sensitivity of photosynthetic functioning to microstructure. Following this, monitoring these aforementioned parameters of photosynthetic function across a longer time span would allow for inference regarding the effect of microstructure on phenology of photosynthetic functioning including photoinhibition (e.g., during early spring when moisture and temperature are limiting but insolation is plentiful). Finally, whereas TLS technology represents the apex of high-resolution structural remote sensing, unmanned aerial systems (i.e., drones) may provide comparable resolution along with substantially broader spatial coverage of the study region.

5. Conclusions

In this study we sought to explore the role of microstructure in explaining variance in photosynthetic functioning (i.e., F_v/F_m) of small-stature spruce trees at the leading edge of the FTE. Our findings demonstrated that trees growing at the FTE are sensitive to fine-scale variability in biophysical structure; using TLS technology for characterizing microstructure, we showed that microstructural metrics alone explained 28% of the variance in photosynthetic functioning of small-stature spruce trees growing at the FTE. The most influential microstructural metrics for explaining variance in photosynthetic functioning were canopy roughness and insolation (when modeled at both the ground surface and the canopy surface). We also demonstrated that the sensitivity of photosynthetic functioning to microstructural metrics is scale-dependent, though the degree to which it is scale-dependent differed by microstructural metric.

The empirical evidence presented here corroborates findings on the importance of microstructure in modulating climatic influence on plant function at treeline ecotones (Scherrer et al., 2011; Scherrer and Körner, 2011, 2010). Our results indicate that high-resolution structural information from remote sensing technology (e.g., lidar or structure-from-motion imagery) may provide valuable insights related to photosynthetic function of trees at the FTE and how variability in microstructure may modulate the coarse-scale effects of climate change. Furthermore, the importance of fine-scale variance in insolation suggests that microstructure may modulate the thermal and light environment conditions to which trees at the FTE are sensitive, particularly during vulnerable development stages. Characterizing the relationships between the remotely sensed structural growth environment and ecological responses is of great interest to broader research endeavors regarding ecological vulnerability at the FTE. This is especially true in the complex biophysical structure inherent to an ecotone. The application of this research will guide future research at the FTE to quantify attributes of biophysical structure that may facilitate the interpretation of physiological dynamics across spatiotemporal scales. In particular, this study demonstrates a means to quantify microstructural attributes that may modulate the response of individual trees at the FTE to coarse-scale climate change. Conclusions from this research will aid in assessing the sensitivity of trees to fine-scale changes in climate and how those fine-scale sensitivities may inform global-scale forest ecosystem modeling under future climate scenarios.

Acknowledgments and author contributions

Funding for this research came from NASA Terrestrial Ecology grant NNX15AT86A and NASA ABoVE grant (Eitel-01). Landscape-scale DEMs were provided by the Polar Geospatial Center under NSF OPP awards 1043681, 1559691 and 1542736. AJM, JUHE, and LAV developed the initial framework and objectives of the study and collected the TLS data. AJM, JUHE, LAV, KLG, NTB, and JEJ contributed to the field data collection. AJM analyzed the data with contributions by JUHE, HEG, and AJHM. AJM drafted the initial version of the manuscript. All co-authors contributed to interpretation of the data and contributed to revisions of the manuscript. The Leica and Trimble instruments were provided by UNAVCO, Inc. (Boulder, CO) and the we are grateful for the technical assistance of Spencer Niebhur. We are grateful for the support provided by the staff of the ABoVE Fairbanks logistics office, notably Sarah Sackett. We would like to thank Dr. Alexander Brenning for his insight on the wind shelter algorithm implemented in RSAGA. We are grateful to Dr. Peter J. Mahoney for his valuable guidance in modeling approaches used and interpretation of the results. Finally, we would like to thank two anonymous reviewers whose careful reading of the initial version of the manuscript improved in clarity of the technical content and message of this manuscript.

References

Anschlag, K., Broll, G., Holtmeier, F.-K., 2008. Mountain birch seedlings in the treeline ecotone, Subarctic Finland: variation in above- and below-ground growth depending on microtopography. Arctic, Antarct. Alp. Res. 40, 609–616. https://doi.org/10.1657/1523-0430(07-087)[ANSCHLAG]2.0.CO;2.

Baig, M.N., Tranquillini, W., 1980. The effects of wind and temperature on cuticular transpiration of Picea abies and Pinus cembra and their significance in dessication damage at the alpine treeline. Oecologia 47, 252–256. https://doi.org/10.1007/BF00346828.

Baker, N.R., 2008. Chlorophyll fluorescence: a probe of photosynthesis in vivo. Annu. Rev. Plant Biol. 59, 89–113. https://doi.org/10.1146/annurev.arplant.59.032607.092759.

Ball, M., Butterworth, J., Roden, J., Christian, R., Egerton, J., Wydrzynski, T., Chow, W., Badger, M., 1995. Applications of chlorophyll fluorescence to forest ecology. Aust. J. Plant Physiol. 22 (311). https://doi.org/10.1071/PP9950311.

Belgiu, M., Drăgu, L., 2016. Random forest in remote sensing: a review of applications and future directions. ISPRS J. Photogramm. Remote Sens. 114, 24–31. https://doi.org/10.1016/j.isprsjprs.2016.01.011.

Bittner, S., Gayler, S., Biernath, C., Winkler, J., Seifert, S., Pretzsch, H., Priesack, E., 2012. Evaluation of a ray-tracing canopy light model based on terrestrial laser scans. Can. J. Remote Sens. 38, 619–628.

Björkman, O., Demmig, B., 1987. Photon yield of O2 evolution and chlorophyll fluorescence characteristics at 77 K among vascular plants of diverse origins. Planta 170, 489–504.

Born, J., Bagchi, R., Burslem, D., Nilus, R., Tellenbach, C., Pluess, A.R., Ghazoul, J., 2015. Differential responses of dipterocarp seedlings to soil moisture and microtopography. Biotropica 47, 49–58. https://doi.org/10.1111/btp.12180.

Breiman, L., 2001. Random forests. Mach. Learn. 45, 5–32. https://doi.org/10.1023/A:1010933404324.

Brenning, A., Bangs, D., 2016. Package 'RSAGA.'.

Brown, D.G., 1994. Predicting vegetation types at treeline using topography and biophysical disturbance variables. J. Veg. Sci. 5, 641–656. https://doi.org/10.2307/3235880.

Callaghan, T.V., Crawford, R.M.M., Eronen, M., Hofgaard, A., Payette, S., Rees, W.G., Skre, O., Sveinbjörnsson, B., Vlassova, T.K., Werkman, B.R., 2002a. The dynamics of the tundra-taiga boundary: an overview and suggested coordinated and integrated approach to research. Ambio 3–5.

Callaghan, T.V., Werkman, B.R., Crawford, R.M.M., 2002b. The tundra-taiga interface and its dynamics: concepts and applications. Ambio 6–14. https://doi.org/10.2307/25094570.

Center, P.G., 2017. Guide: Introduction to ArcticDEM [WWW Document]. URL https://www.pgc.umn.edu/guides/arcticdem/introduction-to-arcticdem/ and be followed by (Accessed 4 February 2018).

Chaudhary, N., Miller, P.A., Smith, B., 2018. Biotic and abiotic drivers of peatland growth and microtopography: a model demonstration. Ecosystems 1–19. https://doi.org/10.1007/s10021-017-0213-1.

Clawges, R., Vierling, L., Calhoon, M., Toomey, M., 2007. Use of a ground-based scanning lidar for estimation of biophysical properties of western larch (Larix occidentalis). Int. J. Remote Sens. 28, 4331–4344. https://doi.org/10.1080/01431160701243460.

Corripio, M.J.G., 2015. Package 'insol.'.

Cutler, D.R., Edwards, T.C., Beard, K.H., Cutler, A., Hess, K.T., Gibson, J., Lawler, J.J., 2007. Random Forests for classification in ecology. Ecology 88, 2783–2792. https://doi.org/10.1890/07-0539.1.

Danby, R.K., Hik, D.S., 2007. Responses of white spruce (Picea glauca) to experimental warming at a subarctic alpine treeline. Glob. Change Biol. 13, 437–451. https://doi.org/10.1111/j.1365-2486.2006.01302.x.

Domènech, M., Komac, B., Peñuelas, J., Conesa, J.A., 2016. Site-specific factors influence the richness and phenology of snowbed plants in the Pyrenees. Plant Biosyst. 150, 741–749. https://doi.org/10.1080/11263504.2014.990941.

Dormann, C.F., Elith, J., Bacher, S., Buchmann, C., Carl, G., Carré, G., Marquéz, J.R.G., Gruber, B., Lafourcade, B., Leitão, P.J., Münkemüller, T., Mcclean, C., Osborne, P.E., Reineking, B., Schröder, B., Skidmore, A.K., Zurell, D., Lautenbach, S., 2013. Collinearity: a review of methods to deal with it and a simulation study evaluating their performance. Ecography 36, 027–046. https://doi.org/10.1111/j.1600-0587.2012.07348.x.

Du, E., 2016. Evidence of soil nutrient availability as the proximate constraint on growth of treeline trees in northwest Alaska: comment. Ecology 97, 801–803.

Eitel, J.U.H., Williams, C.J., Vierling, L.A., Al-Hamdan, O.Z., Pierson, F.B., 2011. Suitability of terrestrial laser scanning for studying surface roughness effects on concentrated flow erosion processes in rangelands. Catena 87, 398–407. https://doi.org/10.1016/j.catena.2011.07.009.

Eitel, J.U.H., Höfle, B., Vierling, L.A., Abellán, A., Asner, G.P., Deems, J.S., Glennie, C.L., Joerg, P.C., LeWinter, A.L., Magney, T.S., Mandlburger, G., Morton, D.C., Müller, J., Vierling, K.T., 2016. Beyond 3-D: the new spectrum of lidar applications for earth and ecological sciences. Remote Sens. Environ. 186, 372–392. https://doi.org/10.1016/j.rse.2016.08.018.

Eitel, J.U.H., Maguire, A.J., Boelman, N., Vierling, L.A., Griffin, K.L., Jensen, J., Magney, T.S., Mahoney, P.J., Meddens, A.J.H., Silva, C., Sonnentag, O., 2019. Remotely sensing tree physiology at northern treeline: do late-season changes in the photochemical reflectance index (PRI) respond to climate or photoperiod? Remote Sens. Environ. 221, 340–350. https://doi.org/10.1016/j.rse.2018.11.022.

Fernández-Marín, B., Atherton, J., Olascoaga, B., Kolari, P., Porcar-Castell, A., García-Plazaola, J.I., 2018. When the sun never sets: daily changes in pigment composition in three subarctic woody plants during the summer solstice. Trees - Struct. Funct. 32, 615–630. https://doi.org/10.1007/s00468-018-1660-9.

Geiger, R., Aron, R.H., Todhunter, P., 2003. The Climate Near the Ground, 6th ed. Rowman & Littlefield Publishers, Inc, Lanham, MD.

Genuer, R., Poggi, J.M., Tuleau-Malot, C., 2010. Variable selection using random forests. Pattern Recognit. Lett. 31, 2225–2236. https://doi.org/10.1016/j.patrec.2010.03.014.

Germino, M.J., Smith, W.K., 1999. Sky exposure, crown architecture, and low-temperature photoinhibition in conifer seedlings at alpine treeline. Plant Cell Environ. 22, 407–415. https://doi.org/10.1046/j.1365-3040.1999.00426.x.

Germino, M.J., Smith, W.K., Resor, A.C., 2002. Conifer seedling distribution and survival in an alpine-treeline ecotone. Plant Ecol. 162, 157–168. https://doi.org/10.1023/A:1020385320738.

Germino, M.J., Hasselquist, N.J., McGonigle, T., Smith, W.K., Sheridan, P.P., 2006. Landscape- and age-based factors affecting fungal colonization of conifer seedling roots at the alpine tree line. Can. J. For. Res. 36, 901–909. https://doi.org/10.1139/x05-303.

Gersony, J.T., Prager, C.M., Boelman, N.T., Eitel, J.U.H., Gough, L., Greaves, H.E., Griffin, K.L., Magney, T.S., Sweet, S.K., Vierling, L.A., Naeem, S., 2016. Scaling thermal properties from the leaf to the canopy in the alaskan arctic tundra. Arctic Antarct. Alp. Res. 48, 739–754. https://doi.org/10.1657/AAAR0016-013.

Greaves, H.E., Vierling, L.A., Eitel, J.U.H., Boelman, N.T., Magney, T.S., Prager, C.M., Griffin, K.L., 2015. Estimating aboveground biomass and leaf area of low-stature Arctic shrubs with terrestrial LiDAR. Remote Sens. Environ. 164, 26–35. https://doi.org/10.1016/j.rse.2015.02.023.

Greaves, H.E., Vierling, L.A., Eitel, J.U.H., Boelman, N.T., Magney, T.S., Prager, C.M., Griffin, K.L., 2016. High-resolution mapping of aboveground shrub biomass in Arctic tundra using airborne lidar and imagery. Remote Sens. Environ. 184, 361–373. https://doi.org/10.1016/j.rse.2016.07.026.

Greaves, H.E., Vierling, L.A., Eitel, J.U.H., Boelman, N.T., Magney, T.S., Prager, C.M., Griffin, K.L., 2017. Applying terrestrial lidar for evaluation and calibration of airborne lidar-derived shrub biomass estimates in Arctic tundra. Remote Sens. Lett. 8, 175–184. https://doi.org/10.1080/2150704X.2016.1246770.

Greenwood, S., Chen, J.C., Chen, C.T., Jump, A.S., 2014. Strong topographic sheltering effects lead to spatially complex treeline advance and increased forest density in a subtropical mountain region. Glob. Change Biol. 20. https://doi.org/10.1111/gcb.12710.

Greenwood, S., Chen, J.-C., Chen, C.-T., Jump, A.S., 2015. Temperature and sheltering determine patterns of seedling establishment in an advancing subtropical treeline. J. Veg. Sci. 26, 711–721. https://doi.org/10.1111/jvs.12269.

Gross, L.J., 1982. Photosynthetic dynamics in varying light environments : a model and its application to whole leaf carbon gain. Ecology 63, 84–93.

Haubrock, S.N., Kuhnert, M., Chabrillat, S., Güntner, A., Kaufmann, H., 2009. Spatiotemporal variations of soil surface roughness from in-situ laser scanning. Catena 79, 128–139. https://doi.org/10.1016/j.catena.2009.06.005.

Hijmans, R.J., 2016. raster: Geographic Data Analysis and Modeling.

Holtmeier, F.-K., 2009. Mountain Timberlines. Springer, Netherlands, Dordrecht. https://doi.org/10.1007/978-1-4020-9705-8.

Holtmeier, F.-K., Broll, G., 1992. The influence of tree islands and microtopography on pedoecological conditions in the forest-alpine tundra ecotone on Niwot Ridge, Colorado front range, U.S.A. Arct. Alp. Res. 24, 216–228.

Holtmeier, F.K., Broll, G., 2005. Sensitivity and response of northern hemisphere altitudinal and polar treelines to environmental change at landscape and local scales. Glob. Ecol. Biogeogr. 14, 395–410. https://doi.org/10.1111/j.1466-822X.2005.00168.x.

Holtmeier, F.K., Broll, G., 2007. Treeline advance - driving processes and adverse factors. Landsc. 1, 1–33. https://doi.org/10.3097/LO.200701. Online.

Holtmeier, F.-K., Broll, G., 2010. Wind as an ecological agent at Treelines in North America, the Alps, and the European subarctic. Phys. Geogr. 31, 203–233. https://doi.org/10.2747/0272-3646.31.3.203.

Holtmeier, F.K., Broll, G., 2017a. Feedback effects of clonal groups and tree clusters on site conditions at the treeline: implications for treeline dynamics. Clim. Res. 73, 85–96. https://doi.org/10.3354/cr01431.

Holtmeier, F.K., Broll, G., 2017b. Treelines-approaches at different scales. Sustainability 9, 1–19. https://doi.org/10.3390/su9050808.

Holtmeier, F.-K., Broll, G., Müterthies, A., Anschlag, K., 2003. Regeneration of trees in the treeline ecotone: Northern Finnish Lapland. Fennia 181, 103–128.

Howe, G.T., Aitken, S.N., Neale, D.B., Jermstad, K.D., Wheeler, N.C., Chen, T.H., 2003. From genotype to phenotype: unraveling the complexities of cold adaptation in forest trees. Can. J. Bot. 81, 1247–1266. https://doi.org/10.1139/b03-141.

Huang, C., Bradford, J.M., 1990. Portable laser scanner for measuring soil surface roughness. Soil Sci. Soc. Am. J. 54, 1402–1406.

Johnson, D.M., Mcculloh, K.A., Reinhardt, K., 2011. The earliest stages of tree growth: development, physiology and impacts of microclimate. In: Meinzer, F.C., Lachenbruch, B., Dawson, T.E. (Eds.), Size- and Age-Related Changes in Tree Structure and Function. Springer, Netherlands, Dordrecht, pp. 65–87. https://doi.org/10.1007/978-94-007-1242-3.

Kambo, D., Danby, R.K., 2018. Factors influencing the establishment and growth of tree seedlings at Subarctic alpine treelines. Ecosphere 9, e02176. https://doi.org/10.1002/ecs2.2176.

Kattsov, V.M., Källén, E., Cattle, H., Christensen, J., Drange, H., Hanssen-bauer, I., Jóhannesen, T., Karol, I., Räisänen, J., Svensson, G., Chen, D., Polyakov, I., Rinke, A., 2005. Future climate change: modeling and scenarios for the Arctic. Arct. Clim. Impact Assess. 99–150.

Körner, C., 1998. A re-assessment of high elevation treeline positions and their explanation. Oecologia 115, 445–459. https://doi.org/10.1007/s004420050540.

Körner, C., 2012. Alpine Treelines: Functional Ecology of the Global High Elevation Tree Limits. Springer, Basel, Switzerland.

Krause, G.H., Weis, E., 1991. Chlorophyll fluorescence and photosynthesis: the basics. Annu. Rev. Plant Physiol. Plant Mol. Biol. 42, 313–349. https://doi.org/10.1146/annurev.pp.42.060191.001525.
Lambers, H., Chapin, F.S.I., Pons, T.L., 2008. Plant Physiological Ecology, 2nd ed. Springer, New York, NY.
Liaw, A., Wiener, M., 2002. Classification and regression by random forest. R news 2/3, 18–22. https://doi.org/10.1177/154405910408300516.
Liaw, A., Wiener, M., 2015. Package "randomForest.".
Magney, T.S., Eusden, S.A., Eitel, J.U.H., Logan, B.A., Jiang, J., Vierling, L.A., 2014. Assessing leaf photoprotective mechanisms using terrestrial LiDAR: towards mapping canopy photosynthetic performance in three dimensions. New Phytol. 201, 344–356. https://doi.org/10.1111/nph.12453.
Magney, T.S., Eitel, J.U.H., Griffin, K.L., Boelman, N.T., Greaves, H.E., Prager, C.M., Logan, B.A., Zheng, G., Ma, L., Fortin, E.A., Oliver, R.Y., Vierling, L.A., 2016. LiDAR canopy radiation model reveals patterns of photosynthetic partitioning in an Arctic shrub. Agric. For. Meteorol. 221, 78–93. https://doi.org/10.1016/j.agrformet.2016.02.007.
Maher, E.L., Germino, M.J., Hasselquist, N.J., 2005. Interactive effects of tree and herb cover on survivorship, physiology, and microclimate of conifer seedlings at the alpine tree-line ecotone. Can. J. For. Res. 35, 567–574. https://doi.org/10.1139/x04-201.
Maxwell, K., Johnson, G.N., 2000. Chlorophyll fluorescence – a practical guide. J. Exp. Bot. 51, 659–668. https://doi.org/10.1093/jexbot/51.345.659.
McNab, W.H., 1996. Ecological Subregions of the United States.
McNown, R.W., Sullivan, P.F., 2013. Low photosynthesis of treeline white spruce is associated with limited soil nitrogen availability in the Western Brooks Range, Alaska. Funct. Ecol. 27, 672–683. https://doi.org/10.1111/1365-2435.12082.
Mesinger, F., DiMego, G., Kalnay, E., Mitchell, K., Shafran, P.C., Ebisuzaki, W., Jović, D., Woollen, J., Rogers, E., Berbery, E.H., Ek, M.B., Fan, Y., Grumbine, R., Higgins, W., Li, H., Lin, Y., Manikin, G., Parrish, D., Shi, W., 2006. North American regional reanalysis. Bull. Am. Meteorol. Soc. 87, 343–360. https://doi.org/10.1175/BAMS-87-3-343.
Millard, K., Richardson, M., 2015. On the importance of training data sample selection in Random Forest image classification: a case study in peatland ecosystem mapping. Remote Sens. 7, 8489–8515. https://doi.org/10.3390/rs70708489.
Nicklen, E.F., Roland, C.A., Ruess, R.W., Schmidt, J.H., Lloyd, A.H., 2016. Local site conditions drive climate-growth responses of Picea mariana and Picea glauca in interior Alaska. Ecosphere 7, e01507. https://doi.org/10.1002/ecs2.1507.
Payette, S., Fortin, M.-J., Gamache, I., 2001. The subarctic forest–tundra: the structure of a biome in a changing climate. Bioscience 51, 709. https://doi.org/10.1641/0006-3568(2001)051[0709:TSFTTS]2.0.CO;2.
Pearcy, R.W., 1990. Sunflecs and photosynthesis in plant life. Annu. Rev. Plant Physiol. Plant Mol. Biol. 41, 421–453. https://doi.org/10.1016/0016-0032(53)91189-2.
Phillips, J.D., 1995. Biogeomorphology and landscape evolution: the problem of scale. Geomorphology 13, 337–347. https://doi.org/10.1016/0169-555X(95)00023-X.
Plattner, C., Braun, L., Brenning, A., 2006. The spatial variability of snow accumulation at Vernagtferner, Austrian Alps, in winter 2003/2004. Zeitschrift für Gletscherkd. und Glazialgeol. 39, 43–57.
Porcar-Castell, A., Tyystjärvi, E., Atherton, J., Van Der Tol, C., Flexas, J., Pfündel, E.E., Moreno, J., Frankenberg, C., Berry, J.A., 2014. Linking chlorophyll a fluorescence to photosynthesis for remote sensing applications: mechanisms and challenges. J. Exp. Bot. 65, 4065–4095. https://doi.org/10.1093/jxb/eru191.
Post, E., Forchhammer, M.C., Bret-Harte, M.S., Callaghan, T.V., Christensen, T.R., Elberling, B., Fox, A.D., Gilg, O., Hik, D.S., Høye, T.T., Ims, R.A., Jeppesen, E., Klein, D.R., Madsen, J., McGuire, A.D., Rysgaard, S., Schindler, D.E., Stirling, I., Tamstorf, M.P., Tyler, N.J.C., van der Wal, R., Welker, J., Wookey, P.A., Schmidt, N.M., Aastrup, P., 2009. Ecological dynamics across the Arctic associated with recent climate change. Science 80 (325). https://doi.org/10.1126/science.1173113. 1355–8.
R Core Team, 2017. R: A Language and Environment for Statistical Computing.
Resler, L.M., 2006. Geomorphic controls of spatial pattern and process at alpine treeline. Prof. Geogr. 58, 124–138.
Resler, L., Butler, D., Malanson, G., 2005. Topographic shelter and conifer establishment and mortality in an alpine environment, Glacier National Park, Montana. Phys. Geogr. 26, 112–125. https://doi.org/10.2747/0272-3646.26.2.112.
Roberts, D.W., Cooper, S.V., 1989. Concepts and techniques of vegetation mapping. In: Ferguson, D., Morgan, P., Johnson, F.D. (Eds.), Land Classification Based on Vegetation: Applications for Resource Management. USDA Forest Service GTR INT-257, Ogden, UT, pp. 90–96.
Ropars, P., Boudreau, S., 2012. Shrub expansion at the foresttundra ecotone: spatial heterogeneity linked to local topography. Environ. Res. Lett. 7. https://doi.org/10.1088/1748-9326/7/1/015501.
Ropars, P., Lévesque, E., Boudreau, S., 2015. How do climate and topography influence the greening of the forest-tundra ecotone in northern Québec? A dendrochronological analysis of Betula glandulosa. J. Ecol. 103, 679–690. https://doi.org/10.1111/1365-2745.12394.
Rosskopf, E., Morhart, C., Nahm, M., 2017. Modelling shadow using 3D tree models in high spatial and temporal resolution. Remote Sens. 9, 719. https://doi.org/10.3390/rs9070719.
Sankey, J.B., Eitel, J.U.H., Glenn, N.F., Germino, M.J., Vierling, L.A., 2011. Quantifying relationships of burning, roughness, and potential dust emission with laser altimetry of soil surfaces at submeter scales. Geomorphology 135, 181–190. https://doi.org/10.1016/j.geomorph.2011.08.016.
Scherrer, D., Körner, C., 2010. Infra-red thermometry of alpine landscapes challenges climatic warming projections. Glob. Change Biol. 16, 2602–2613. https://doi.org/10.1111/j.1365-2486.2009.02122.x.
Scherrer, D., Körner, C., 2011. Topographically controlled thermal-habitat differentiation buffers alpine plant diversity against climate warming. J. Biogeogr. 38, 406–416. https://doi.org/10.1111/j.1365-2699.2010.02407.x.
Scherrer, D., Schmid, S., Körner, C., 2011. Elevational species shifts in a warmer climate are overestimated when based on weather station data. Int. J. Biometeorol. 55, 645–654. https://doi.org/10.1007/s00484-010-0364-7.
Serreze, M.C., Walsh, J.E., Chapin III, F.S., Osterkamp, T., Dyurgerov, M., Romanovsky, V., Oechel, W.C., Morison, J., Zhang, T., Barry, R.G., 2000. Observational evidence of recent change in the northern high-latitude environment. Clim. Change 46, 159–207. https://doi.org/10.1023/A:1005504031923.
Shaver, G.R., Laundre, J.A., Giblin, A.E., Nadelhoffer, K.J., 1996. Changes in live plant biomass, primary production, and species composition along a Riverside Toposequence in Arctic Alaska, U.S.A. Arct. Alp. Res. 28, 363–379.
Shepard, M.K., Campbell, B.A., Bulmer, M.H., Farr, T.G., Gaddis, L.R., Plaut, J.J., 2001. The roughness of natural terrain: a planetary and remote sensing perspective. J. Geophys. Res. Planets 106, 32777–32795. https://doi.org/10.1029/2000JE001429.
Skre, O., Baxter, R., Crawford, R.M.M., Callaghan, T.V., Fedorkov, A., 2002. How will the tundra-taiga interface respond to climate change? Ambio 37–46. https://doi.org/10.2307/25094574.
Slot, M., Wirth, C., Schumacher, J., Mohren, G.M.J., Shibistova, O., Lloyd, J., Ensminger, I., 2005. Regeneration patterns in boreal Scots pine glades linked to cold-induced photoinhibition. Tree Physiol. 25, 1139–1150. https://doi.org/10.1093/treephys/25.9.1139.
Smith, W.K., Berry, Z.C., 2013. Sunflecks? Tree Physiol. 33, 233–237. https://doi.org/10.1093/treephys/tpt005.
Smith, W.K., Knapp, A.K., Reiners, W.A., 1989. Penumbral effects on sunlight penetration in plant communities. Ecology 70, 1603–1609.
Smith, W.K., Germino, M.J., Hancock, T.E., Johnson, D.M., 2003. Another perspective on altitudinal limits of alpine timberlines. Tree Physiol. 23, 1101–1112.
Stoner, W.A., Miller, P.C., 1975. Water relations of plant species in the wet coastal tundra at Barrow, Alaska. Arct. Alp. Res. 7, 109–124. https://doi.org/10.1657/1523-0430(06-007.
Sullivan, P.F., 2016. Evidence of soil nutrient availability as the proximate constraint on growth of treeline trees in northwest Alaska: reply. Ecology 97, 803–808.
Sullivan, P.F., Sveinbjörnsson, B., 2010. Microtopographic control of treeline advance in noatak national preserve, Northwest Alaska. Ecosystems 13, 275–285. https://doi.org/10.1007/s10021-010-9318-5.
Sullivan, P.F., Ellison, S.B.Z., McNown, R.W., Brownlee, A.H., Sveinbjornsson, B., 2015. Evidence of soil nutrient availability as the proximate constraint on growth of treeline trees in northwest Alaska. Ecology 96, 716–727. https://doi.org/10.1890/14-0626.1.
Sveinbjörnsson, B., Hofgaard, A., Lloyd, A., 2002. Natural causes of the tundra-taiga boundary. Ambio 23–29. https://doi.org/10.2307/25094572.
Tranquillini, W., 1979. Physiological ecology of the alpine timberline. Ecological Studies, 1st ed. Springer, Berlin Heidelberg, Berlin, Heidelberg. https://doi.org/10.1007/978-3-642-67107-4.
Trant, A.J., Hermanutz, L., 2014. Advancing towards novel tree lines? A multispecies approach to recent tree line dynamics in subarctic alpine Labrador, northern Canada. J. Biogeogr. 41. https://doi.org/10.1111/jbi.12287.
Vitasse, Y., Lenz, A., Kollas, C., Randin, C.F., Hoch, G., Körner, C., 2014. Genetic vs. non-genetic responses of leaf morphology and growth to elevation in temperate tree species. Funct. Ecol. 28, 243–252. https://doi.org/10.1111/1365-2435.12161.
Way, D.A., Pearcy, R.W., 2012. Sunflecks in trees and forests: from photosynthetic physiology to global change biology. Tree Physiol. 32, 1066–1081. https://doi.org/10.1093/treephys/tps064.
Widlowski, J.-L., Côté, J.-F., Béland, M., 2014. Abstract tree crowns in 3D radiative transfer models: impact on simulated open-canopy reflectances. Remote Sens. Environ. 142, 155–175. https://doi.org/10.1016/j.rse.2013.11.016.
Winstral, A., Elder, K., Davis, R.E., 2002. Spatial snow modeling of wind-redistributed snow using terrain-based parameters. J. Hydrometeorol. 3, 524–538. https://doi.org/10.1175/1525-7541(2002)003<0524:SSMOWR>2.0.CO;2.
Woods, K.D., 2014. Problems with edges: tree lines as indicators of climate change (or not). Appl. Veg. Sci. 17, 4–5. https://doi.org/10.1111/avsc.12077.
Yang, Z., Sykes, M.T., Hanna, E., Callaghan, T.V., 2012. Linking fine-scale sub-arctic vegetation distribution in complex topography with surface-air-temperature modelled at 50-m resolution. Ambio 41, 292–302. https://doi.org/10.1007/s13280-012-0307-0.
Zong, S., Wu, Z., Xu, J., Li, M., Gao, X., He, H., Du, H., Wang, L., 2014. Current and potential tree locations in tree line ecotone of Changbai Mountains, Northeast China: the controlling effects of topography. PLoS One 9. https://doi.org/10.1371/journal.pone.0106114.